Generation of Pretilt Angle and an Alignment Layer Utilizing Binary Mixture in PI-less Vertical Alignment Mode

Gwan Yong Lee[1], Jun Hyeok Lee[1], Seong Min Song[1], Ramesh Manda[1], Young Jin Lim[1], Seung Hee Lee[1]*

[1]Applied Materials Institute for BIN Convergence, Department of BIN Convergence Technology and Department of Polymer Nano-Science and Technology, Jeonbuk National University, Jeonju, Jeonbuk 54896, Korea

Abstract

We demonstrate new approach of polyimide (PI)-less polymer stabilized vertical alignment (PS-VA) mode in which binary mixture of single kind of reactive mesogen and LC induces a VA with temperature treatment. The induced VA is fixed at first UV exposure and then a pretilt angle is generated with second UV exposure. The proposed device with two-step UV exposure exhibits excellent electro-optics such as fast response time and enhanced on-state transmittance. This approach fixes a vertical alignment physically unlike chemical bonding in conventional PI-less VA mode, giving rise to high reliability.

Author Keywords

Vertical alignment; PS-VA; Polyimide-less; Reactive Mesogen

1. Introduction

LCDs with VA mode are widely used in LCD-TVs owing to its advantage in achieving an excellent dark state, giving rise to a high contrast ratio over 5000: 1. Varies kinds of VA modes had been proposed based on novel electrode structure and manipulation of pretilt angles. In general, a polyimide (PI) with high density of side chains is used to generate a very stable vertical alignment [1]. However, a rather complicated coating process with thickness of less than 100 nm is required and then curing process above 200 ^{o}C, which is high-cost and time- consuming process [2-3]. In order to overcome the above- mentioned disadvantages, an alignment layer-free techniques such as optically isotropic liquid crystal (OILC) using either blue phase or nano-sized LC droplet have been challenged, however, they are not commercialized yet [4]. Recently, PI-less methods for both vertical alignment [5] and homogenous alignment [6,7] have been challenged. Especially, for polymer stabilized (PS)-VA mode, two dopants (LC with polar OH for hydrogen bonding to surfaces and reactive mesogen (RM)) are doped into LC and once a vertical alignment is induced a bias voltage is applied and then UV is exposed to generate a pretilt angle by polymer stabilization of RM [8,9]. Therefore, choosing right materials for VA inducer and pretilt angle generation determines electro-optic performance of PI-less VA mode and its sustainability and reliability. In addition, conventional VA inducer is chemically bonded to the substrates, which may exhibit not stable enough vertical alignment. Considering the next-generation VA display devices, there is a necessity of improving this device further.

In this paper, we demonstrate new approach of PI-less PS-VA mode in which single RM is doped into LC and two-step UV curing process is performed to fix vertical alignment and generate pretilt angle. The proposed device performs excellent electro-optics. This approach is having a great advantage of simplified process by reducing processing steps and cost effectiveness.

2. Mechanism and Materials

The schematic of the proposed device is illustrated in **Fig. 1**. At initial state, both LC and RM molecules are randomly located all over the cell area. Next, a thermal treatment is performed by keeping the sample at 80 ^{o}C above T_{ni} for 5 min. During the long thermal treatment, the RM molecules move towards the substrate's surface and orient orthogonal to the substrate due to long thermal stress, thereby extend the orientation into the bulk LC up to some extent. And in next stage, the RM is cured through the UV curing (first cure), forms a surface localized polymer layer. Now, the cell is cool down to room temperature and an electric field is biased between two substrates (patterned electrode on bottom and plane electrode on top substrate) to orient LC in a desired direction. When the high electric field is applied, the LC molecules, mostly at center of the cell, reorients perpendicular to the electric field (i.e. parallel to the substrate) with well-defined azimuthal angles. At this stage, a secondary UV curing was performed under electric field applied. Through this process, the residual RM is cured to generate pretilt angle for LC alignment even after field removal.

In this study, a PS-VA device is comprised of a nematic LC with negative dielectric anisotropy, ZSM-7125 (T_{NI} = 76.0 ^{o}C, Δn = 0.101 at 25 ^{o}C, n_e = 1.583, n_o = 1.482, $\Delta\varepsilon$ = -2.90, from JNC Corporation, from Japan), and a RM, UCL-M3 (DIC corporation, Japan). The LC to RM ratio is fixed to 98.8:1.2. In order to achieve a uniform mixture, the RM is added to LC at its isotropic temperature and performed a vertex mixing for 5 min. Next, the homogeneous mixture of LC and RM is infiltrated into experimental cell by capillary action at 80 ^{o}C.

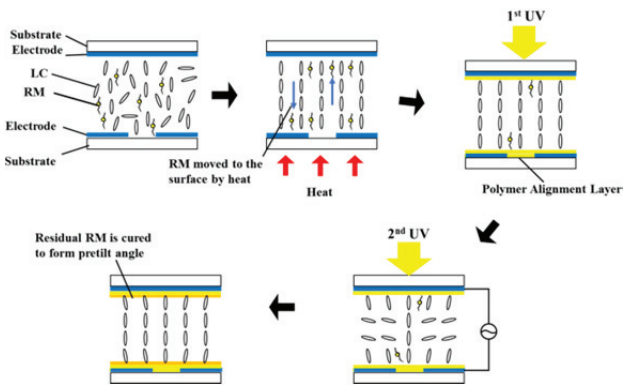

Figure 1. Schematic diagram of manufacturing PI-less PS- VA mode LC cell.

3. Results and Discussions

The schematic structure of the two-domain experimental cell is shown in **Fig. 2**. The bottom substrate consists of patterned electrodes while top substrate consists of non-patterned plane ITO. The microscopic images of the bottom substrate with 200x and 500x magnification is shown in **Fig. 2(a)** and **Fig. 2(b)**, respectively. Both width and separation of electrodes is measured to be 3 μm and the cell gap is fixed to 3.1 μm.

 ISSN 0097-996X/20/4803-1982-$1.00 © 2020 SID

Firstly, an essential characterizations are performed after LC infiltration. As one can easily notice from macroscopic bulk images and the POM images in Fig. 3(a) and (b), the LC molecules are randomly oriented although there is a small indication of LC orientation in the flow direction of infiltration. The macroscopic images were recorded by taking high resolution photographs when the sample placed between the crossed polarizers and appropriate backlight is illuminated.

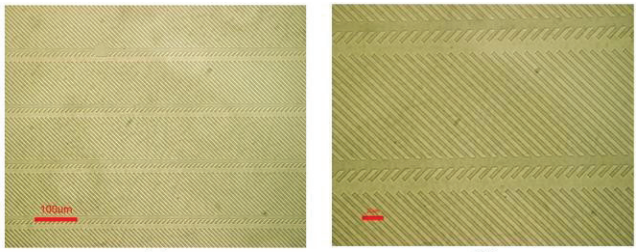

Figure 2. Optical microscope images of two-domain LC with magnification, (a) 200x and (b) 500x.

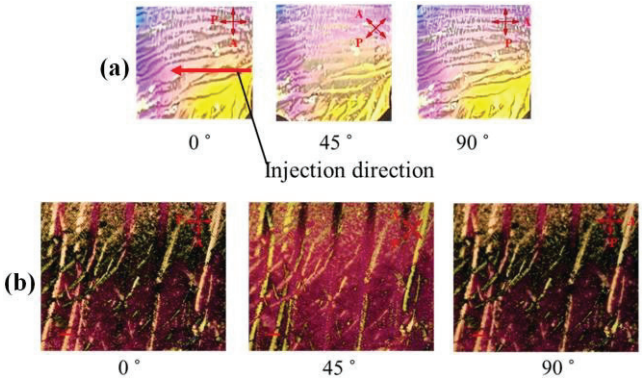

Figure 3. (a) Macroscopic and (b) POM images before heat treatment.

Next, we have performed a heat treatment to the sample by keeping the cell at 80 ^{o}C for 5 min. Figure 4(a)-4(c) shows a macroscopic, POM, and conoscopy images of the sample after thermal treatment, respectively. The obtained results suggest that there is no indication of light leakage through crossed polarizers. In addition, the conoscopy images suggests that the LC molecules are oriented perpendicular to the substrate. We presume that the RM was moved to the surface of the substrate through heat treatment and induced vertical alignment to the bulk LC. The long-term thermal curing could produce the thermal stress which causes RM molecules verticle alignment transfers into LC up to some extent.

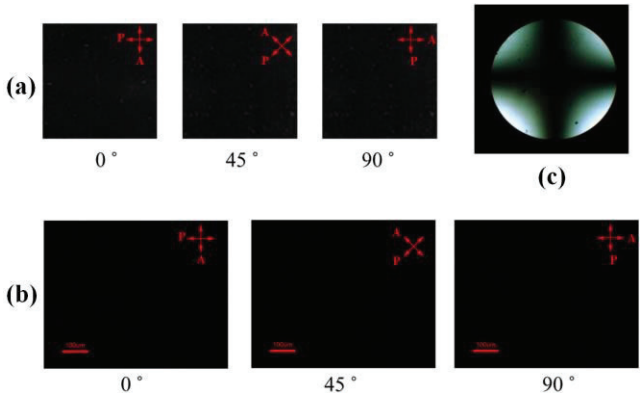

Figure 4. After heat treatment of cell, (a) Macroscopic, (b) POM, and (c) conoscopy images.

In a next step, the UV curing was performed to the sample by irradiating 10mW/cm^2 UV light for 80s and subsequent characterizations are performed, as shown in **Fig. 5**. It is interesting to notice that the dark state is unaltered by UV irradiation. And the conoscpic data indicates that the vertical alignment of LC is unaltered after RM polymerization. From **Fig. 5(a)** and **5(b)**, we have also noticed that the images exhibit a light leakages similar to those in **Fig. 4**.

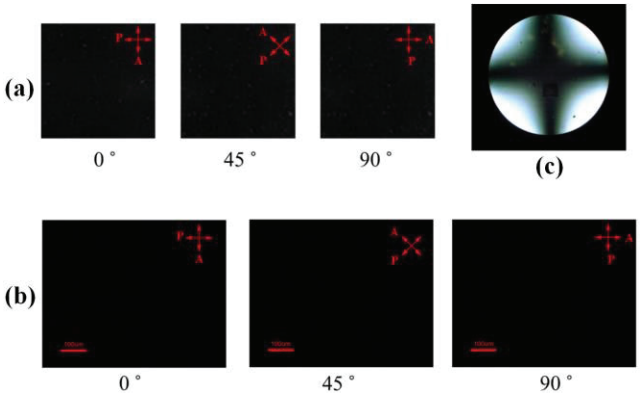

Figure 5. (a) Macroscopic, (b) POM, and (c) conoscopy images of cells after first UV curing.

Through the first UV curing, the RM forms a surface localized polymer alignment layer so that the LC can be switched well by an electric field, that is, LC can relax back to original VA quickly in the absence of an electric field. Here, electro-optic characterizations are performed by applying square wave voltage. The threshold voltage and the operating voltage were confirmed by measuring the voltage-dependent transmittance curve. As shown in the Fig. 6, the threshold voltage and the operating voltage were measured as 2.5 V and 5.2 V, respectively.

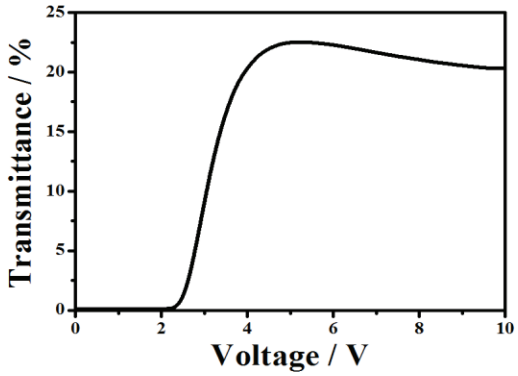

Figure 6. Voltage-dependent transmittance curve after first UV curing.

By applying the voltage corresponding to the operating voltage, i.e., 5.2 V, the time-resolved LC texture are observed through the POM. Fig. 7 shows the sequence of LC textures in response to the electric field. The disclinations or defects are clearly evident in the textures during the field-induced reorientation as depicted in **Fig. 7**. It suggests that the LC does not have defined azimuthal angle to tilt down due to absence of pretilt angle. These POM textures are analogue to conventional VA mode where the on- state LC orientation is random or undefined due to absence of pretilt angle. Consequently, it takes more than a second for the LC texture to be stabilized.

Further, the response time was measured to check the LC orientation and relaxation dynamics. Fig. 8 shows the rise and decay time of the first UV cured cell, which are 251.7 ms and 29.2 ms, respectively. We assume that the longer rise time is resultant from unknown preferred on-state orientational direction due to absence of pretilt. Thus, the second UV curing was performed to form the pretilt angle of the LC during applying operating voltage that gives a clear bright state without LC textures.

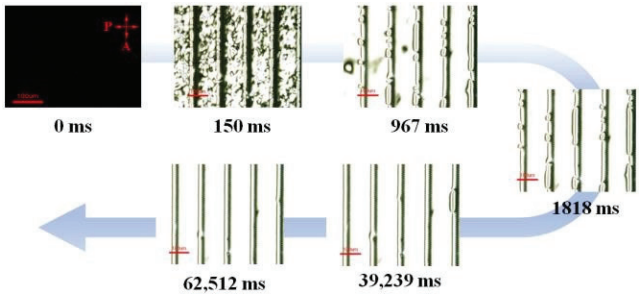

Figure 7. Time-resolved LC texture of the first UV cured cell.

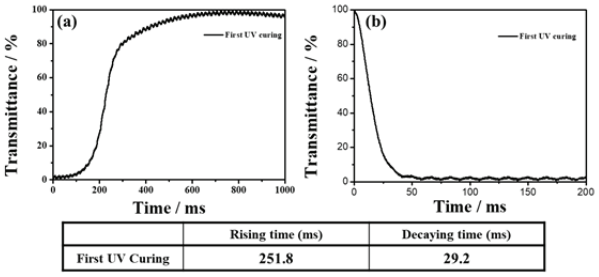

	Rising time (ms)	Decaying time (ms)
First UV Curing	251.8	29.2

Figure 8. (a) Rise time and (b) decay time of the sample after first UV curing.

Fig. 9 shows macroscopic, POM and conoscopic images of cells after the second UV curing at 10 mW/cm^2 for 500 s. It shows that the dark state is still unchanged even after second UV curing but the conoscopic image breaks slightly show four-fold symmetry unlike the one in the first cured cell. In other words, orientation of the LC molecules is unaltered by second UV curing, exhibiting a dark level similar to the Fig. 5, however, a pretilt angle is formed.

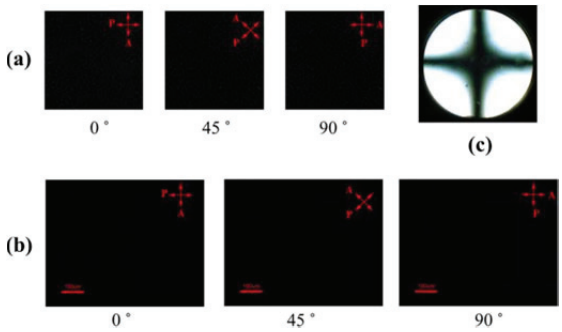

Figure 9. (a) Macroscopic, (b) polarized optical microscopy, and (c) conoscopy images of cells after second UV curing.

We expect that through the second UV curing, the residual RM is cured to form additional polymer layer. Since UV curing was performed under the applied electric field, the liquid crystal has a slight pretilt angle like conventional PS-VA mode. In order to confirm the pretilt angle of the liquid crystal, the V-T curve was measured first.

Fig. 10 shows the V-T curve of the cell after the second UV curing, which shows that the threshold and operating voltages are 2.5 V and 4.4 V, respectively. Overall, V-T curve shifts to the left, which is clear indicator of existence of the pretilt angle. In addition, the increase in transmittance 3% of second UV curing curve is obtained from the second curing.

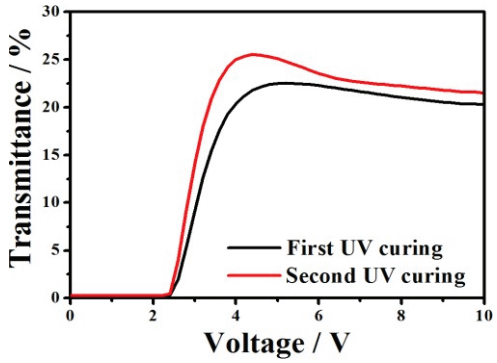

Figure 10. Voltage-transmittance curve of the second UV cured cell.

To confirm, the time-resolved LC textures were observed in the POM by applying the operating voltage of 4.4 V, as shown in Fig. 11. Unlike those in Fig. 7, the LC stabilization time become much quicker and there shows no LC texture during reorientation, clearly indicating that the pretilt angle of the LC is formed. To confirm more clearly, the response time was measured, as shown in Fig. 12. The rise and decay times are 12.6 ms and 25.1 ms, respectively. The rise response time is considerably reduced than that of the first UV cured cell, which means that a pretilt angle is formed. Interestingly, the decay time becomes shorter too. We expect the anchoring force is strengthened through the second UV while removing residual RMs in a bulk LC. Through this result, we conclude we successfully manufactured the PI-less PS-VA mode.

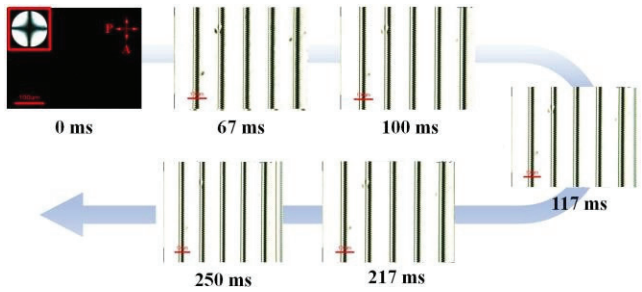

Figure 11. Time-resolved LC texture of the second UV cured cell.

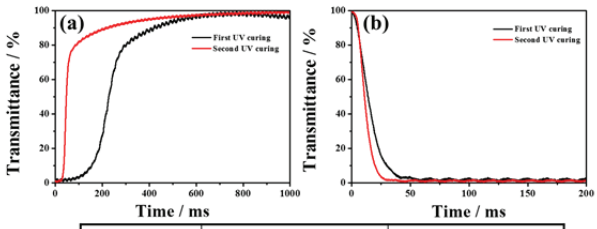

	Rising time (ms)	Decaying time (ms)
First UV Curing	251.8	29.2
Second UV Cuing	12.7	25.2

Figure 12. (a) Rise time and (b) decay time of the second UV cured cell.

3. Impact

We propose PI-less PS-VA mode that forms vertical alignment as well as a controllable pretilt angle by adopting two-step UV curing approach. Unlike ternary mixture and chemical bonding induced vertical alignment in the conventional PI-less VA device, our is utilizing binary mixture and physical bonding for vertical alignment. The proposed PS-VA mode device is exhibiting excellent electro-optics such as the fast response time and high on-state transmittance. In addition, the device is having a great advantage of less material consumption and significantly reduces the processing steps. These results are expected to significantly increase the productivity of the VA-LCD mode. The thermal and UV reliability comparison between ours and conventional approach is under test.

4. Acknowledgements

This research was supported by the Basic Science Research Program through the National Research Foundation of Korea (NRF) funded by the Ministry of Education (2016R1D1A1B01007189) and by the National Research Foundation of Korea (NRF) grant founded the Korea government (MSIT) (No. 2019R1A5A8080326)

5. References

[1] J. M. Geary, J. W. Goodby, A. R. Kmetz, & J. S. Patel, “The mechanism of polymer alignment of liquid-crystal materials”, J. Appl. Phys., 62, 4100, (1987)

[2] Hoogboom, J., Rasing, T., Rowan, A. E., & Nolte, R. J. M. “LCD alignment layers. Controlling nematic domain properties”, J. Mater. Chem., 16(14), 1305-131, (2006).

[3] Jiao, M., Ge, Z., Song, Q., & Wu, S.-T. “Alignment layer effects on thin liquid crystal cells”. Applied Physics Letters, 92(6), 061102 (2008).

[4] Y. J. Lim, J. H. Yoon, H. -S. Yoo, S. M. Song, R. Manda, S. Pagidi, M. -H. Lee, J. -M. Myoung, and S. H. Lee “Fast switchable field-induced optical birefringence in highly transparent polymerliquid crystal composite”, Optical Material Express, 8(12), 3698-9707, (2018).

[5] S. -C. Jeng, C. -W. Kuo, H. -L. Wang, and C. -C. Liao, “Nanoparticles-induced vertical alignment in liquid crystal cell,” Appl. Phys. Lett. 91, 061112 (2007).

[6] Y. Wang, C. Xu, A. Kanazawa, T. Shiono, T. Ikeda, Y. Matsuki, & Y. Takeuchi, “Thermal stability of alignment of a nematic liquid crystal induced by polyimides exposed to linearly polarized light”. Liq Cryst, 28(3), 473-475, (2018).

[7] R. He, P. Wen, S. -W. Kang, S. H. Lee, & M.-H. Lee “Polyimide-free homogeneous photoalignment induced by polymerizable liquid crystal containing cinnamate moiety.”. Liq. Cryst., 45(9), 1-11, (2018).

[8] I. T. Son, C. H. Kim, J. H. Kin, B. S. Lee, J. Y. Yoo, & J. H. Lee, “Fabrication of a new homeotropic alignment layer for nematic liquid crystals using an in situ self-assembly of alkylated benzoic acid derivative”, Mol. Cryst. Liq. Cryst., 644(1), 98-102, (2017)

[9] Q. Li, Y. Zhang, H.-Q. Wei, W. Cui, T.-J. Tseng, C.-C. Hsieh, C.-Y. Chiu, “Study on the effect of controlling the pretitle angle using RM with multipolymerizable functional group”. SID Symposium Digest of Technical Papers, 27(1), 371–374, (2019)